Light-driven progesterone production by InP-(M. neoaurum) biohybrid system

Kun Liu
East China University of Science and Technology
Feng-Qing Wang (fqwang@ecust.edu.cn)
East China University of Science and Technology https://orcid.org/0000-0002-3473-5991
Ke Liu
East China University of Science and Technology
Yunqiu Zhao
East China University of Science and Technology
Bei Gao
East China University of Science and Technology
Xinyi Tao
East China University of Science and Technology
Dongzhi Wei
East China University of Science and Technology

Research Article

Keywords: Synthetic biology, Progesterone, P450, Electron transfer, InP nanoparticles, NADPH/NADP+

Posted Date: June 1st, 2022

DOI: https://doi.org/10.21203/rs.3.rs-1663838/v1

Abstract

Progesterone is one of the classical hormone drugs used in medicine for maintaining pregnancy. However, its manufacturing process, coupled with organic reagents and poisonous catalysts, results in irreversible environmental pollution. Recent advances in synthetic biology have demonstrated the microbial biosynthesis of natural products, especially difficult-to-synthesize compounds, synthetic from building blocks is a promising strategy. Herein, overcoming the heterologous cytochrome P450 enzyme interdependency in *Mycolicibacterium neoaurum* successfully constructed the CYP11A1 running module to realize the metabolic conversion from waste phytosterols to progesterone. Subsequently, progesterone yield was improved through strategies involving electron transfer and NADPH regeneration. The CYP11A1 and ADR were connected by a flexible linker as a chimera to enhance electron transfer. Strain MNR-08 showed positive activity, with 45 mg/L progesterone, leading to a 3.95-fold improvement over strain MNR-04. Significantly, a novel inorganic-biological hybrid system was assembled by combining MNR-08 and InP nanoparticles to regenerate NADPH, which was increased 84-fold from the initial progesterone titers to 235 ± 50 mg/L. Altogether, this work highlights the green and sustainable potential for synthetic progesterone from sterols in *M. neoaurum*.

Introduction

Progesterone (4-Pregnen-3,20-Dione) is a natural progestational hormone necessary for maintaining pregnancy. It not only plays an important role in the reproductive system, such as hormone regulation and sexual response (Mulac-Jericevic et al. 2000), but also has applications in the respiratory, central nervous, and urinary systems. Traditionally, progesterone is synthesized from the precursor “diosgenin”, which is extracted from plants (such as ginger). There are two main routes to synthesize progesterone or other steroid hormones: Route 1 is a “diosgenin to diene” (Hanson 2005; Donova & Egorova 2012), and this route involves multistep chemical reactions and microbial transformation processes for the degradation of diosgenin to produce steroid drugs. Another route is “sterol conversion” (Yao et al. 2014; Zhou et al. 2020; Feng et al. 2022), in which diosgenin is used as substrate and transformed into steroid intermediates, and subsequently, by complicated chemical methods, steroid drugs are obtained. These routes inevitably cause environmental pollution, are nongreen, are noneconomical, are toxic, waste fresh water resources, and consume unpredictable organic compounds and heavy metals; thus, a green and sustainable concept of biotechnology (Langsdorf et al. 2021) needs to be developed to produce steroid drugs.

Phytosterols (PS) were transformed by *Mycolicibacterium neoaurum* to produce 22-hydroxy-23,24-bisnorchol-4-ene-3-one (HBC), which is a key intermediate in the synthesis of progesterone through two-step chemical reactions: the oxidation of HBC to HBC aldehyde and the copper-mediated catalytic radical oxygenation of aldehyde to progesterone (Sun et al. 2019; Peng et al. 2021). Although this strategy simplifies the synthesis of progesterone from diosgenin, it still uses hazardous chemical reagents, such as 2,2'-bipyridine. Fortunately, we found that HBC has a low Michaelis constant (Km) for bovine CYP11A1 (P450 monooxygenase) (Table S3), perhaps because they have a similar steroidal ring, and its C22 has a

hydroxyl. Thus, we inferred that CYP11A1 had highly efficient activity catalyzing HBC into progesterone and that progesterone was directly produced from the biodegradation of phytosterols by *M. neoaurum* fermentation. Typically, CYP11A1 is the key enzyme that catalyzes cholesterol (ChO) into pregnenolone (Duport et al. 1998) and this reaction, along with 3 O_2 and 3 NADPH, is consumed in classical steroidogenic glands (Bernhardt & Urlacher 2014). In particular, previous works (Guengerich 2001; Strushkevich et al. 2011) shed light on the catalytic mechanism of CYP11A1, in which the reactions involved initial hydroxylation at C22 and C20, producing 22R-hydroxycholesterol and 20R,22R-dihydroxycholesterol, respectively. This 20R,22R-dihydroxycholesterol is followed by oxidative cleavage of the C20-C22 bond, resulting in the formation of a carbonyl for pregnenolone. Based on this mechanism, studies performed over a number of years have demonstrated that a range of substrates can be transformed into novel CYP11A1-derived secosteroids. These analog substrates included 7-dehydrocholesterol (Guryev et al. 2003) and ergosterol (Slominski et al. 2005), which were converted into 7-dehydropregnenolone and pregnenolone by purified CYP11A1, respectively. Unfortunately, CYP11A1 activities are lower than expected, mainly because it has heterologous expression interdependency and requires adrenodoxin (ADX) and adrenodoxin reductase (ADR) to transfer electrons (Grinberg et al. 2000). To overcome CYP11A1 interdependency, Irina A. Pikuleva and coworkers (Pikuleva 2004) identified the putative F-G loop of CYP11A1 associated with membrane attachment. Furthermore, a single amino acid mutation, truncation of the N-terminal, and deletion of the F-G loop together successfully resulted in an approximately 4-fold increase in solubility in *E. coli* JM 109 (Janocha et al. 2011). Although these strategies conquered membrane anchoring to realize free expression in the cytoplasm, CYP11A1 activities were still not high. The low activity might be due to that inefficient of the electron transfer protein interaction with CYP11A1 (Sagadin et al. 2018). Additionally, bovine CYP11A1 and ADX in the reaction system work quite well, but bovine ADR can also be a problem because its expression in bacteria is very difficult (Gerber et al. 2015). Therefore, this system should attempt to other reductases that support its correct reaction and easy to expression in bacteria. Moreover, the efficiency of electron transfer to the overall P450 activities is very often overlooked, and a promising strategy for improving product titers is the optimization of electron flow (Liu & Yu 2020; Song et al. 2021). A protein chimera was applied to the field of a bioenzymatic successfully (Gao et al. 2014). Therefore, a flexible chimera was employed to accelerate electron transfer from NADPH to the substrate, since this chimera shortened the distance and improved random collision or interactions between CYP11A1 and ADR.

It is another challenge for P450 reactions and/or metabolism involving cofactors, namely, nicotinamide adenine dinucleotide (NADH) or its phosphorylated form (NADPH), because the cofactor is expensive and its involved reactions produce further waste byproducts (Wang et al. 2013). Regardless of enzymatic or electrochemical regeneration of NAD(P)H, $NAD(P)^+$ is reduced to NAD(P)H due to $NAD(P)^+$ obtaining a hydride ion [H^-, (H^++2e^-)], whereas the protonation rate of the $NAD(P)^+$ radicals is less than its radical form, leading to inactive 1,6-NAD(P)H and $NAD(P)_2$ dimers (Kohlmann et al. 2008; Liu et al. 2018). These methods would aggravate the metabolic burden for the troublesome P450 and cycle-limiting regeneration of NAD(P)H. Fortunately, inorganic-biological hybrid systems (Sakimoto et al. 2015; Brown et al. 2016; Hu et al. 2021) have established the electron donation capabilities of illuminated semiconductors to

regenerate cofactors. Indium phosphide (InP) nanoparticles were selected as a semiconductor photosensitizer in biohybrid systems because they enable absorption of a greater fraction of the solar spectrum and accept electrons from various microorganisms in the liquid medium (Guo et al. 2018). It is possible that InP-(*M. neoaurum*) biohybrids both intensify the efficiency of NADPH regeneration and lead to the enhanced biosynthesis of steroids.

In view of the above challenges, sterol conversion, a green and an effective strategy, can be directly performed in *M. neoaurum* to obtain progesterone from sterols. Herein, we demonstrate production of progesterone via *M. neoaurum* in which the core step is biotransformation of HBC to progesterone using bovine CYP11A1, thereby enabling the direct production of progesterone from PS (Fig. 1). CYP11A1 expression was optimized including N-terminal truncation, pivotal F-G loop deletion and site mutation (Pikuleva 2004; Janocha et al. 2011; Gerber et al. 2015); and successfully expressed in *M. neoaurum* and exhibited positive enzyme activity. Subsequently, to overcome CYP11A1 interdependency with its partners to further improve progesterone titers, screening of redox partners and construction of enzyme chimeras were used as methods to accelerate electron transfer. Last, in the context of semiconductor light-harvesting InP nanoparticles, decoupling NADPH regeneration from central carbon metabolism facilitated the production of progesterone. This report provides a new *M. neoaurum* for the production of a certain steroid drug, progesterone, from sterols.

Material And Methods

Chemicals and reagents

Phytosterols (more than 95%, w/w) (Yao et al. 2013), including campesterol 26.4%, beta-sitosterol 47.5%, stigmasterol 17.7%, and brassicasterol 3.6%, were purchased from Sciphar Natural Products Co., Ltd. (Shanxi, China). Cholesterol, progesterone, tannic acid, poly(allylamine hydrochloride) (PAH) and pregnenolone were supplied by Sigma–Aldrich (Shanghai, China). HBC and InP (3–20 mesh) were obtained from Steraloids (Newport, RI, USA) and Aladdin (Shanghai, China), respectively. HP-β-CD (hydroxypropyl-β-cyclodextrin) was obtained from RSC Chemical Industries Co., Ltd. (Kunshan, China). Other chemicals and reagents were supplied by companies with reagent grade or the highest purity available.

FastDigest restriction enzymes were purchased from Fermentas (ThermoFisher, USA). High-fidelity DNA polymerase and NAD(P)H detection kits were obtained from Solarbio Science & Technology Co., Ltd. (Beijing, China). The intracellular concentrations of NADPH and $NADP^+$ were determined in a similar method to how NADH was determined by zhang (Zhang et al. 2009; Zhao et al. 2019). The plasmid extraction kit and gel extraction kit were supplied by Magen Biotech Co., Ltd. (Shanghai, China). A one-step cloning kit was purchased from Yeasen Biotech Co., Ltd. (Shanghai, China).

PS mother liquor (100 g/L) was prepared by mixing phytosterols (20 g), hydroxypropyl-β-cyclodextrin (80 g), and water (100 mL). Then, this turbid liquid was stirred and sonicated to make smaller size

phytosterols. Finally, the mother liquor was fixed to 200 ml and sterilized at 121 ℃ for 21 min. ChO and HBC mother liquor (100 g/L) were prepared by the same method.

Strains, plasmids and primers

For details, please see Table S1 and Table S2. *M. neoaurum* ATCC 25795 was isolated from a soil sample using steroids as a single carbon source, which were sterol consumers with no metabolic pathways in detail. Based on the original strain *M. neoaurum* ATCC 25795, the genes *KstD* (3-ketosteroid-Δ^1-dehydrogenase), *KSH* (9α-hydroxylase), *Hsd4A* (17β-hydroxysteroid dehydrogenase), and *FadA5* (encoding a thiolase) were deleted to produce HBC (Xu et al. 2016), and HBC accumulated in the fermentation medium as a major product of the *M. neoaurum*.

Medium and culture conditions

The inoculum was cultured in Luria-Bertani (LB) medium (tryptone 10 g/L, yeast extract 5 g/L, NaCl 10 g/L) or LB plate medium with 1.8% agar. The optimum flask medium (MNR01) was employed as a preliminary experiment in shake flasks, containing 20 g/L glycerol, 2 g/L citric acid monohydrate, 0.5 g/L $K_2HPO_4{\cdot}3H_2O$, 0.5 g/L $MgSO_4{\cdot}7H_2O$, 2.52 g/L KNO_3, 1.65 g/L $(NH_4)_2HPO_4$, and 0.05 g/L ammonium ferric citrate with an initial pH of 7.5-8.0. The fermentation medium (MNR02) consisted of 10 g/L glucose, 2.5 g/L citric acid monohydrate, 0.5 g/L $K_2HPO_4{\cdot}3H_2O$, 0.5 g/L $MgSO_4{\cdot}7H_2O$, 3.5 g/L $(NH_4)_2HPO_4$, and 0.05 □/L ammonium ferric citrate and was maintained at pH 7.0 with 2 M NaOH. The MNR01 and MNR02 media were sterilized at 121 ℃ for 21 min and 115 ℃ for 30 min, respectively.

A loopful of MNR glycerol stocks was inoculated into LB plates at 30 ℃ for approximately 4–6 days. Then, the MNR colonies were picked and cultured in a 20 mL shake flask containing 5 mL of LB medium with 50 μg/mL kanamycin (Kan) for plasmid selection at 30 ℃ for approximately 2–3 days with shaking at 200 rpm. Primary seed inocula (10%, v/v) were added into a 250 mL shake flask with 30 mL MNR01 medium at 30 ℃ with shaking at 200 rpm until the optical density was not less than 4 at 600 nm. Finally, the secondary inocula (10%, v/v) were harvested from the 250 mL flask fermentation broth and used to convert sterols. With respect to biohybrid transformation, 20 g/L resting cells converted 5 g/L substrates into progesterone in pH 7.4 phosphate buffered saline (PBS) buffer under light-emitting diode (LED) power in the rotater at 30 ℃ with 200 rpm.

Construction of the bacterial operons and strains

All cDNA genes were obtained from NCBI Reference, including bovine CYP11A1 (NP_788817.1), bovine AdR (NP_777116.1), bovine Adx (NP_851354.1), yeast ARH1 (AJV00869.1), and porcine ADR (NP_001231656.1). These genes were codon-optimized for *Mycobacterium* and completely synthesized by Genscript (China). In addition, the *g6pdh* gene was amplified from the genome of *M. neoaurum* ATCC 25795. To achieve prosperous translation in *M. neoaurum*, multiple genes were expressed in tandem by a bacterial operon in the shuttle vector pMV261, and there were stop codon TGA and RBS sequences between two adjacent genes. In addition, the linkage of gene fragments in an operon was determined using fusion polymerase chain reaction (PCR). The amplified operons were then ligated to pMV261,

which was successively digested by Msc I and Sal I to form the recombinant plasmid pMV261. Table S1 shows the main recombinant plasmid pMV261 used in this study.

The recombinant plasmid pMV261 with different synthetic bacterial operons was transformed into competent DH5α cells. Then, the recombinant pMV261s were extracted from DH5α cells, and their DNA sequences were sequenced. Finally, these correct recombinant plasmids were electrotransformed into MNRs, and the empty vector pMV261 was also transformed into MNRs as a control. The positive recombinant strains were screened, the presence of their heterologous genes was ensured by PCR, and the strains were kept in 20% glycerol at -80 ℃.

Steroid extraction and analysis

To extract progesterone from the fermentation broth, a 2- to 3-fold volume of ethyl acetate was added to the broth. The broth was dried, oscillated for 3 to 5 min, and centrifuged at 8000 rpm for 5 min. Finally, the above organic phase was transferred to an empty tube and volatilized in a fume cupboard to remove ethyl acetate, so isopycnic methanol was added to the tube again. Samples and standards were dotted on silica gel plates (Macklin Biochemical Co., Ltd., Shanghai, China), where the developing solvent was an organic mixture of petroleum ether and ethyl acetate (3:2), sprayed with 20% H_2SO_4, and subsequently oxidized at 105 ℃ for 15–20 min for thin layer chromatography (TLC) analysis.

UHPLC–MS (Mass Spectrometer, Q Exactive Orbitrap, Thermo-Fisher Scientific, USA) analysis was carried out both in full scan and electron spray ionization (ESI) source by scanning all the ions of the products. Data were acquired with a Surveyor Autosampler and MS Pump and analyzed with Xcalibur software (Thermo-Fisher Scientific, USA). The product, progesterone, from transformant conversion was confirmed with sample MS analysis and standard (progesterone) MS comparison. The ethyl acetate extract was separated and purified to obtain a collected liquid of progesterone by silica gel column chromatography. Then, the organic solvent was removed from the collected liquid by spin evaporation. The residual substance after spin evaporation was dissolved in methanol, and this saturated progesterone solution was placed in a -40 ℃ refrigerator to crystallize pure progesterone. Finally, ^{1}H-NMR and ^{13}C-NMR (Solution, methanol-d_4) spectra were obtained on a Bruker (Ascend 600 MHz) nuclear magnetic resonance (NMR) spectrometer. The quantification of progesterone was performed by high-performance liquid chromatography (HPLC, Agilent 1260). The separation conditions included ZORBAX SB C18 (4.6 * 250 mm, particle size 5 nm, Agilent), CH_3OH and H_2O (8:2), 20 μL sample injection, 1 mL/min flow rate, 30 ℃ column temperature, and an absorbing wavelength of 242 nm.

InP–(M. neoaurum) biohybrid assembly

Indium phosphide nanoparticles were obtained through manual grinding. Field emission scanning electron microscopy (SEM) images were obtained on a GeminiSEM 500 (Germany) to test nanoparticle size, operating at an accelerating voltage of 1 ~ 15 kV. The assembly method of InP on cells was based on modified positively charged polymers, poly (allylamine hydrochloride)-containing InP nanoparticles, which were used to adsorb on the *M. neoaurum* surface (Guo et al. 2016). Its morphology was observed

by high-resolution transmission electron microscopy (TEM, JEM-2100, Japan). During the assembly process, the operation of mixing the suspension of nanoparticles and cells is described in literature appendix (Guo et al. 2018).

Results And Discussion

Overcoming CYP11A1 interdependency: heterologous expression in M. neoaurum

A great deal of P450 heterologous expression involves membrane-bound and specific electron transfer protein(s); in addition, most available methods have difficulty overcoming interdependency. To date, scientists have developed a set of promising devices that combine truncated membrane attachment with directed evolution to obtain free and hydrophilic P450s and successfully increase P450 enzyme activities in multiple hosts (Biggs et al. 2016; Zhang et al. 2019). A simple investigation of free-expressing bovine CYP11A1 was carried out in the chassis, and combined with truncated and site-mutated amino acids, CYP11A1 was found to realize free-expressing CYP11A1 (Fig. S2). Concretely, N-terminal truncation, F-G loop deletion, and site mutation K193E of CYP11A1 were modified, but the conservative amino acids of the region of ADX binding to CYP11A1 (465R, 466R) ensured consistency (Fig. S1). In addition, genes with a high GC (65–70%) almost consistent with the chassis (~ 66.7%) were also optimized, and software predicted that its mRNA secondary structure was simpler, with less hairpin and higher free energy, indicating that mutant *cyp11a1 (mcyp11a1)* translation would be easier. The mCYP11A1 was free and soluble, indicating that production of progesterone has achieved the first step in the P450 module for *M. neoaurum* metabolic conversion. The P450 module was added downstream of producing HBC (Fig. 1) and was found to inhibit *M. neoaurum* growth and decrease HBC titers (unpublished data). The introduction of multiple plasmids pMV261 with different resistance resulted in metabolic burden (Karim et al. 2013), the plasmid burdensome pathway was subjected to unknown inactivation, and the introduction of a multiple plasmid system aggravated this burden, especially for the troublesome metabolism of P450. Additionally, the genome editing tools of *M. neoaurum* are immature so that multiple genes cannot be localized to multiple sites, only the *attB* site. Therefore, to avoid multiplasmid system metabolic burden, the P450 module pathway involving enzymes was tandemly expressed in a bacterial operon (Fig. 2a).

Subsequently, to test CYP11A1 module metabolic pathway running status, the substrates PS and ChO were added into flasks for fermentation respectively. The metabolite progesterone was initially analyzed and compared by chromatography. ChO was used as a substrate because the conversion rate of its utilization by MNRs is higher than that of PS, making it easier to analyze the target product (Fig. S3 and Fig. 4b). Compared with the position of standard progesterone, the Rf and RT corresponding to the dots and peaks of the new product are consistent with the standard progesterone (Fig. S4). More interestingly, HBC was added to medium and fermented by MNR-03, merely expressing mCYP11A1 in the MNR was found that can convert HBC into progesterone. The cause might be that the chassis has soluble electron carriers from NADPH-dependent reductase to P450, which has the same function for transmitting electrons as ADR and ADX. To address this discovery theoretically, *M. neoaurum* has diversiform P450s

(~ 30) and electron carriers (Liu et al. 2018). In addition, the natural redox partners of P450s are mostly unknown, and P450s can also accept electrons from the other partners (Sagadin et al. 2018). In practice, class I P450 enzymes that catalyze steroids abide by the following reaction (Sadeghi & Gilardi 2013):

Through the quantitative relationship between produced progesterone and intracellular consumed NADPH revealed the existence of unknown electron carriers consistent with ADR and ADX functions in MNRs. The results suggested that the ratio of progesterone to NADPH (1:3.125) was close to the theoretical value of 1:3 (Fig. 2b-c). Therefore, this result indicated abundant P450 enzymes and electron carriers in MNRs support electron transfers for CYP11A1. In total, *M. neoaurum* has the advantage of transporting electrons between NADPH and CYP11A1 and overcame the interdependence of CYP11A1 with the native host.

Identification of biotransformation products

The bioconversion products, using HBC and ChO as substrates, were further characterized by high-resolution mass spectrometry (HRMS). Figure 3 shows the HRMS results that the mass-to-charge ratios of the bioconversion products progesterone and pregnenolone were 314 m/z and 316 m/z, respectively, and these products were equal to preestablished standards (Fig. S11-13). To further confirm the structure of the product, the isolated and purified product was used for structural identification by NMR, and ^{1}H-NMR and ^{13}C-NMR suggested that this product was progesterone (Fig. S14-15). In addition, pregnenolone was thought to be the main product of CYP11A1 transforming ChO because reports have confirmed that CYP11A1 converts ChO to pregnenolone (Makeeva et al. 2013; Strizhov et al. 2014; Gerber et al. 2015). Unexpectedly, the HPLC results suggested that progesterone was the main product and that pregnenolone was an intermediate from ChO to progesterone. Therefore, HBC was catalyzed by CYP11A1 to produce progesterone and that ChO is directly metabolized into progesterone by MNR-04. With respect to pregnenolone, one hypothesis is that 3β-HSD (3beta-hydroxysteroid dehydrogenase) catalyzes C3 dehydrogenation from pregnenolone, leading to the production of progesterone (Szczebara et al. 2003; Xu et al. 2016). In total, progesterone was directly obtained in engineered *M. neoaurum* from PS through metabolic flux modulation.

Driven intermolecular electron transfer by flexible chimera

To address intermolecular electron transfer for P450, reports mainly have four classes of alternative approaches to enhance electron transfer, including screening of redox partners, artificial fusion chimera, and light-activation as well as electrochemical reductions. With respect to screening redox partners, it is very difficult to establish high-throughput screening technology. Therefore, expressing known oxidoreductase chaperones was chosen, such as porcine ADR (MNR-05) pADR) and *S. cerevisiae* ARH1 (MNR-06), for which the former showed negative titers, but the latter showed positive activities (Fig. 4a). This result may be because ARH1 is an adrenodoxin reductase-related homolog derived from microbes

that is more easily and correctly expressed in bacteria. Furthermore, the rat CYP1A1-cytochrome P450 reductase (CPR) fusion protein, the first microsomal P450-CPR fusion protein, was successfully constructed by Murakami et al. in 1987 (Murakami et al. 1987) indicating efficient electron transfer between domains within artificial fusion, and this strategy could be a promising application in biotechnology. Subsequently, many reports studied P450 electron transfer using artificial fusion, which included bovine CYP17A1-Rat CPR (Fisher et al. 1992) and CYP3A4-BMR (Dodhia et al. 2008). Without the exception of CYP11A1, Jennifer and coworkers (Harikrishna et al. 1993) constructed three fusion proteins and transfected them into COS-1 cells; only the CYP11A1-ADR-ADX fusion protein produced substantially more pregnenolone. In contrast, the artificial chimera CYP11A1-L-ADR (MNR-07) showed positive activity, 16.8 mg/L progesterone, leading to an over 1.47-fold improvement over MNR-04. The direct fusion of CYP11A1-ADR could impact the interactions of domains; however, the linker [L: $(GGGGS)_2$] (Chen et al. 2013) provided flexibility and allowed for mobility of the connecting functional domains, resulting in close and correct domains based on native interactions of CYP11A1 and ADR. The close and correct domains indicated that their electron transfer would yield more effectivity and activity. ADX exhibits a cytosolic distribution and is easily expressed in bacteria (Gerber et al. 2015), so ADX probably collides and interacts with CYP11A1, causing electron transfer from ADX to CYP11A1. Therefore, the construction of chimera CYP11A1-L-ADR-L-ADX would not significantly improve the effectivity of electron transfer. In addition, electron flow was enhanced by overexpressing ARH1, which can supply electrons for CYP11B1 to enhance steroid production and promote metabolic flow toward hydrocortisone (Szczebara et al. 2003). The electron flow was enhanced through coexpression of ARH1 in MNR-08 so that the progesterone titer reached 24 mg/L. To further improve the progesterone titer, PS and ChO were compared by resting cells of MNR-08 (Caro et al. 2007; Wu et al. 2017; Zhang et al. 2020), and 45 mg/L progesterone was obtained using 5 g/L ChO as a substrate for fermentation (Fig. 4b), which was 16.1 times higher than the initial concentration. However, the transformation of sterols into progesterone did not abide by mass balance; progesterone increased by approximately 20 mg/L, leading to its precursor HBC decreasing by more than 20 mg/L (progesterone/HBC = 330/314 ≈ 1/1, w/w) (Fig. 4a). This result was caused by 3 product-related aspects, including bacteriostasis, decomposition, and feedback inhibition (Fig. S5-6). As we reported previously, inhibition of yeast growth by progesterone caused a sharp drop in fluorescence intensity (Liu et al. 2022). These problems are expected to be solved later from product separation in situ and stress screening.

Preparation and characterization of the biohybrid system

InP nanoparticles between 20–500 nm with negative charges are important for the realization of biohybrid systems. Therefore, 3–20 mesh InP powders were manually ground in a mortar for 20–40 min to obtain nanoparticles with diameters less than 500 nm. The ground InP powders were washed three times with ddH_2O and then dispersed into suspension by ultrasound for 15 min. After being centrifuged and attached to the tube wall, the InP particles were characterized to determine their size by SEM (Fig. 5a). Then, InP nanoparticles and tannic acid solutions were mixed to form an inorganic nanoparticle suspension. Polyphenol-functionalized InP nanoparticles were incubated with 70% ethanol for 10 min and washed with ddH_2O 3 times. TEM images show that tannic acid and InP formed supramolecular

networks on the surface of the InP nanoparticles (Fig. 5b). This result indicated that the negatively charged tannic acid made the surface of InP nanoparticles negatively charged. Sonication was applied to disperse the polyphenol-functionalized InP nanoparticles in the suspension to obtain monodispersity of the nanoparticles for uniform adsorption on the cell surface.

It is essential that the cell surface with a positive charge realize electrostatic adsorption for the assembly process of biohybrids. Logarithmically metaphase-engineered *M. neoaurum* was harvested and washed with PBS 3 times. Positively charged PAH was mixed with cells so that PAH was used to adsorb on the surface of the cell. The functionalized cells were washed with ddH_2O three times to remove unabsorbed PAH. The assembly process of biohybrids can occur after mixing polyphenol-functionalized InP nanoparticles with PAH-functionalized cells. TEM images show that InP nanoparticles with negative charges were adsorbed on the surface of cells with positive charges (Fig. 6B). Figure 6a suggests that 20 mM InP nanoparticles easily form a barrier equivalent to cell wall thickening and cause difficulties in substrate uptake and electron transfer. However, the surface of cells cannot adsorb sufficient nanoparticles (Fig. 6c), indicating that photoelectric conversion is inefficient from the surface to the cytoplasm. Combined with Fig. S7, Fig. 6b was chosen as assembled biohybrids of resting cell fermentations because the surface of the cells was evenly coated with nanoparticles.

Decoupling NADPH regeneration by light-driven electron transport

Figure 2b-c shows that exogenous addition of NADPH can improve the progesterone titer. Additionally, coupling NADPH regeneration was used as a common approach, such as overexpression glucose-6-phosphate dehydrogenase (G6PDH), which faces byproducts requiring downstream separation and limited regeneration numbers. The intracellular NADPH/$NADP^+$ ratio was maintained at a relatively low level by overexpression of G6PDH, and only 29 mg/L progesterone was produced (Fig. S8). In contrast, decoupling NADPH generation from other metabolites may be a possibility for a great deal of production of desired products and lower byproducts (Wang et al. 2017; Guo et al. 2018). A novel method was attempted that light-driven NADPH regeneration in biohybrids of *M. neoaurum*, where InP light-harvesting semiconductor nanoparticles attached to the surface of bacteria were able to provide reducing equivalents to central metabolic processes (Sakimoto et al. 2015). In other words, electrons flowing from illuminated MNR-surface-bound InP to $NADP^+$ inside the bacteria regenerated NADPH (Fig. 1). A high availability of cytosolic NADPH via photon energy conversion (Xu et al. 2019) directly facilitates the production of progesterone, and this method-produced progesterone titer should be higher than that overexpressing G6PDH. The effect of light on steroid products was investigated by illuminating resting MNR-InP transforming ChO (Fig. 7a). The results shown that light-on not only enhanced the titer of progesterone but also strengthened the titer of the intermediate HBC, which indicated that the illuminated semiconductor can not only transfer electrons for $NADP^+$ but also provide electrons for other substances in the cell (Fig. S10). This conclusion is consistent with the energy-efficient production of the metabolite shikimic acid and its precursor 3-dehydroshikimic acid (Guo et al. 2018).

To identify whether the progesterone increase was due to $NADP^+$ reduction, the NADPH/$NADP^+$ ratio was tested in cytosolic MNR-InP. Figure 7b shows the highest NADPH/$NADP^+$ ratios in the light-on system. These results support that illuminated *M. neoaurum* surface-assembled InP nanoparticles can drive NADPH regeneration in the cytoplasm and enhance steroid production. However, it was hard to achieve complete darkness in a shaker, which was the cause of the also-increasing steroid yield with lights off. There was another hypothesis for the increased steroid production. PAH functionalization, such as functionalized PHB (poly(3-hydroxybutyrate), is crucial for the high conversion rate by serving as steroid storage, which may mean that the degradation of progesterone is reduced (Gerber et al. 2015). Additionally, the biotransformation trended to a dynamic balance, and the ratio of NADPH/$NADP^+$ decreased after 5 d of fermentation, mainly due to the thickening of the cell wall making electron transfer difficult, and the efficiency of substrate uptake and product efflux decreased. Similarly, too much polyphenol-functionalized InP adsorbed on the surface of MNR-08 to form a dense barrier, similar to a thickened cell wall, which hindered electron transfer (Fig. 6a and Fig. S7). Fig. S9 suggested that brighter light did not lead to an increase in progesterone production but affected the metabolism of steroids and gave rise to cell metabolism disorders. It was also reported that strong light destroyed the cell wall and inhibited the metabolism of the bacteria (Wang et al. 2021). In summary, the illuminated MNR-InP biohybrids drive intracellular NADPH regeneration and facilitate sterol conversion, resulting in a progesterone titer up to 235 ± 50 mg/L, which is 5.2-fold higher than that of MNR-08.

Conclusions

A green and sustainable approach was established to produce progesterone directly from sterols via the addition of a bovine P450 module in *M. neoaurum*. Concretely, overcoming the heterologous interdependency between CYP11A1 and reductase partners, and it was successfully expressed in *M. neoaurum* to obtain an initial progesterone titer of 2.8 mg/L. To enhance the progesterone titer, strategies optimization of electron flow and light-driven NADPH regeneration were used together led to an 84-fold increase in yield by resting conversion, up to 235 ± 50 mg/L. These conclusions provide a perspective to promote metabolic efficiency for other low-efficiency P450s.

Declarations

Author contributions

Kun Liu: Conceptualization, methodology, software, investigation, writing; Feng-Qing Wang: supervision, funding acquisition, conceptualization, re-writing; Ke Liu and Yunqiu Zhao: validation; Bei Gao and Xinyi Tao: supervision; Dongzhi Wei: supervision, funding acquisition.

Acknowledgements

Not applicable

Funding

This work was financially supported by the National Natural Science Foundation of China (Grant No. 21776075).

Ethics approval and consent to participate

Not applicable.

Consent for publication

All the authors consent to the publication of this manuscript.

Availability of data and materials

All data generated or analysed during this study are included in this article (and its additional information files).

Competing interests

The authors declare no competing interests.

References

1. Bernhardt R, Urlacher VB (2014) Cytochromes P450 as promising catalysts for biotechnological application: chances and limitations. Appl Microbiol Biotechnol 98(14):6185–6203.
2. Biggs BW, Lim CG, Sagliani K, Shankar S, Stephanopoulos G, De Mey M, Ajikumar PK (2016) Overcoming heterologous protein interdependency to optimize P450-mediated taxol precursor synthesis in *Escherichia coli*. Proc Natl Acad Sci U S A 113(12):3209–3214.
3. Brown KA, Harris DF, Wilker MB, Rasmussen A, Khadka N, Hamby H, Keable S, Dukovic G, Peters JW, Seefeldt LC, King PW (2016) Light-driven dinitrogen reduction catalyzed by a CdS:nitrogenase MoFe protein biohybrid. Science 352(6284):448–450.
4. Caro A, Boltes K, Letón P, García-Calvo E (2007) Dibenzothiophene biodesulfurization in resting cell conditions by aerobic bacteria. Biochem Eng J 35(2):191–197.
5. Chen X, Zaro JL, Shen W (2013) Fusion protein linkers: Property, design and functionality. Adv Drug Deliv Rev 65(10):1357–1369.
6. Dodhia VR, Sassone C, Fantuzzi A, Nardo GD, Sadeghi SJ, Gilardi G (2008) Modulating the coupling efficiency of human cytochrome P450 CYP3A4 at electrode surfaces through protein engineering. Electrochem commun 10(11):1744–1747.
7. Donova MV, Egorova OV (2012) Microbial steroid transformations: current state and prospects. Appl Microbiol Biotechnol 94(6), 1423–1447.
8. Duport C, Spagnoli R, Degryse E, Pompon D (1998) Self-sufficient biosynthesis of pregnenolone and progesterone in engineered yeast. Nat Biotechnol 16(2):186–189.

9. Feng J, Wu Q, Zhu D, Ma Y (2022) Biotransformation enables innovations toward green synthesis of steroidal pharmaceuticals. ChemSusChem.
10. Fisher CW, Shet MS, Caudle DL, Martin-Wixtrom CA, Estabrook RW (1992) High-level expression in *Escherichia coli* of enzymatically active fusion proteins containing the domains of mammalian cytochromes P450 and NADPH-P450 reductase flavoprotein. Proc Natl Acad Sci U S A 89(22):10817–10821.
11. Gao X, Yang S, Zhao C, Ren Y, Wei D (2014) Artificial multienzyme supramolecular device: highly ordered self-assembly of oligomeric enzymes in vitro and in vivo. Angew Chem Int Ed 53(51):14027–14030.
12. Gerber A, Kleser M, Biedendieck R, Bernhardt R, Hannemann F (2015) Functionalized PHB granules provide the basis for the efficient side-chain cleavage of cholesterol and analogs in recombinant *Bacillus megaterium*. Microb Cell Fact 14(1).
13. Grinberg AV, Hannemann F, Schiffler B, Muller J, Heinemann U, Bernhardt R (2000) Adrenodoxin: structure, stability, and electron transfer properties. Proteins 40(4):590–612.
14. Guengerich FP (2001) Common and uncommon cytochrome P450 reactions related to metabolism and chemical toxicity. Chem Res Toxicol 14(6):611–650.
15. Guo J, Suastegui M, Sakimoto KK, Moody VM, Xiao G, Nocera DG, Joshi NS (2018) Light-driven fine chemical production in yeast biohybrids. Science 362(6416):813–816.
16. Guo J, Tardy BL, Christofferson AJ, Dai Y, Richardson JJ, Zhu W, Hu M, Ju Y, Cui J, Dagastine RR, Yarovsky I, Caruso F (2016) Modular assembly of superstructures from polyphenol-functionalized building blocks. Nat Nanotechnol 11(12):1105–1111.
17. Guryev O, Carvalho RA, Usanov S, Gilep A, Estabrook RW (2003) A pathway for the metabolism of vitamin d3: unique hydroxylated metabolites formed during catalysis with cytochrome P450scc (CYP11A1). Proc Natl Acad Sci U S A 100(25):14754–14759.
18. Hanson JR (2005) Steroids: reactions and partial synthesis. Nat Prod Rep *22*(1):104.
19. Harikrishna JA, Black SM, Szklarz GD, Miller WL (1993) Construction and function of fusion enzymes of the human cytochrome P450scc system. DNA Cell Biol 12(5):371–379.
20. Hu G, Li Z, Ma D, Ye C, Zhang L, Gao C, Liu L, Chen X (2021) Light-driven CO_2 sequestration in *Escherichia coli* to achieve theoretical yield of chemicals. Nat Catal 4(5):395–406.
21. Janocha S, Bichet A, Zöllner A, Bernhardt R (2011) Substitution of lysine with glutamic acid at position 193 in bovine CYP11A1 significantly affects protein oligomerization and solubility but not enzymatic activity. Biochim Biophys Acta Proteins Proteom 1814(1):126–131.
22. Karim AS, Curran KA, Alper HS (2013) Characterization of plasmid burden and copy number in *Saccharomyces cerevisiae* for optimization of metabolic engineering applications. FEMS Yeast Res 13(1):107–116.
23. Kohlmann C, Märkle W, Lütz S (2008) Electroenzymatic synthesis. J Mol Catal B Enzym 51(3–4):57–72.

24. Langsdorf A, Volkmar M, Holtmann D, Ulber R (2021) Material utilization of green waste: a review on potential valorization methods. Bioresour Bioprocess 8(19):1–26.
25. Liu K, Zhang Y, Liu K, Zhao Y, Gao B, Tao X, Zhao M, Wang F, Wei D (2022) De novo design of a transcription factor for a progesterone biosensor. Biosens Bioelectron 203, 113897.
26. Liu M, Xiong L, Tao X, Liu Q, Wang F, Wei D (2018) Integrated transcriptome and proteome studies reveal the underlying mechanisms for sterol catabolism and steroid production in *Mycobacterium neoaurum*. J Agric Food Chem 66(34):9147–9157.
27. Liu X, Yu X (2020) Enhancement of butanol production: from biocatalysis to bioelectrocatalysis. ACS Energy Lett 5(3):867–878.
28. Liu X, Shi L, Gu J (2018) Microbial electrocatalysis: redox mediators responsible for extracellular electron transfer. Biotechnol Adv 36(7):1815–1827.
29. Makeeva DS, Dovbnya DV, Donova MV, Novikova LA (2013) Functional reconstruction of bovine P450scc steroidogenic system in *Escherichia coli*. Am J Mol Biol 03(04):173–182.
30. Mulac-Jericevic B, Mullinax RA, DeMayo FJ, Lydon JP, Conneely OM (2000) Subgroup of reproductive functions of progesterone mediated by progesterone receptor-B isoform. Science 289(5485):1751–1754.
31. Murakami H, Yabusaki Y, Sakaki T, Shibata M, Ohkawa H (1987) A genetically engineered P450 monooxygenase: construction of the functional fused enzyme between rat cytochrome P450c and NADPH-cytochrome P450 reductase. DNA 6(3):189–197.
32. Peng H, Wang Y, Jiang K, Chen X, Zhang W, Zhang Y, Deng Z, Qu X (2021) A dual role reductase from phytosterols catabolism enables the efficient production of valuable steroid precursors. Angew Chem Int Ed 60(10):5414–5420.
33. Pikuleva IA (2004) Putative F-G loop is involved in association with the membrane in P450scc (P450 11A1). Mol Cell Endocrinol *215*(1–2):161–164.
34. Sadeghi SJ, Gilardi G (2013) Chimeric P450 enzymes: Activity of artificial redox fusions driven by different reductases for biotechnological applications. Biotechnol Appl Biochem 60(1):102–110.
35. Sagadin T, Riehm JL, Milhim M, Hutter MC, Bernhardt R (2018) Binding modes of CYP106A2 redox partners determine differences in progesterone hydroxylation product patterns. Commun Biol 1(1).
36. Sakimoto KK, Wong AB, Yang P (2015) Self-photosensitization of nonphotosynthetic bacteria for solar-to-chemical production. Science 351(6268):74–77.
37. Slominski A, Semak I, Zjawiony J, Wortsman J, Gandy MN, Li J, Zbytek B, Li W, Tuckey RC (2005) Enzymatic metabolism of ergosterol by cytochrome p450scc to biologically active 17α,24-dihydroxyergosterol. Chem Biol, 12(8):931–939.
38. Song Z, Wei C, Li C, Gao X, Mao S, Lu F, Qin H (2021) Customized exogenous ferredoxin functions as an efficient electron carrier. Bioresour Bioprocess 8(109):1–13.
39. Strizhov N, Fokina V, Sukhodolskaya G, Dovbnya D, Karpov M, Shutov A, Novikova L, Donova M (2014) Progesterone biosynthesis by combined action of adrenal steroidogenic and mycobacterial

enzymes in fast growing *Mycobacteria*. New Biotechnol 31:S67.

40. Sun W, Wang L, Liu H, Liu Y, Ren Y, Wang F, Wei D (2019) Characterization and engineering control of the effects of reactive oxygen species on the conversion of sterols to steroid synthons in *Mycobacterium neoaurum*. Metab Eng 56:97–110.
41. Szczebara FM, Chandelier C, Villeret C, Masurel A, Bourot S, Duport C, Blanchard S, Groisillier A, Testet E, Costaglioli P, Cauet G, Degryse E, Balbuena D, Winter J, Achstetter T, Spagnoli R, Pompon D, Dumas B (2003) Total biosynthesis of hydrocortisone from a simple carbon source in yeast. Nat Biotechnol 21(2):143–149.
42. Wang X, Li J, Zhang C, Zhang Y, Meng J (2021) Self-assembly of CdS@*C. Beijerinckii* hybrid system for efficient lignocellulosic butanol production. Chem Eng J 424:130458.
43. Wang X, Saba T, Yiu HHP, Howe RF, Anderson JA, Shi J (2017) Cofactor NAD(P)H regeneration inspired by heterogeneous pathways. Chem 2(5):621–654.
44. Wang Y, San KY, Bennett GN (2013) Cofactor engineering for advancing chemical biotechnology. Curr Opin Biotechnol 24(6):994–999.
45. Wu J, Ng I (2017) Biofabrication of gold nanoparticles by *Shewanella* species. Bioresour Bioprocess 4(50):1–9.
46. Xu L, Liu Y, Yao K, Liu H, Tao X, Wang F, Wei D (2016) Unraveling and engineering the production of 23,24-bisnorcholenic steroids in sterol metabolism. Sci Rep 6(1).
47. Xu M, Tremblay P, Jiang L, Zhang T (2019) Stimulating bioplastic production with light energy by coupling Ralstonia eutropha with the photocatalyst graphitic carbon nitride. Green Chem 21(9):2392–2400.
48. Yao K. Wang F, Zhang H, Wei D (2013) Identification and engineering of cholesterol oxidases involved in the initial step of sterols catabolism in *Mycobacterium neoaurum*. Metab Eng 15:75–87.
49. Yao K, Xu L, Wang F, Wei D (2014) Characterization and engineering of 3-ketosteroid-$\triangle^1$-dehydrogenase and 3-ketosteroid-9α-hydroxylase in *Mycobacterium neoaurum* ATCC 25795 to produce 9α-hydroxy-4-androstene-3,17-dione through the catabolism of sterols. Metab Eng 24:181–191.
50. Zhang RK, Chen K, Huang X, Wohlschlager L, Renata H, Arnold FH (2019) Enzymatic assembly of carbon-carbon bonds via iron-catalysed sp3 C-H functionalization. Nature 565(7737):67–72.
51. Zhang X, Peng Y, Zhao J, Li Q,Yu X, Acevedo-Rocha CG, Li A (2020) Bacterial cytochrome P450-catalyzed regio- and stereoselective steroid hydroxylation enabled by directed evolution and rational design. Bioresour Bioprocess 7(2):1–18.
52. Zhang Y, Huang Z, Du C, Li Y, Cao ZA (2009) Introduction of an NADH regeneration system into *Klebsiella oxytoca* leads to an enhanced oxidative and reductive metabolism of glycerol. Metab Eng 11(2):101–106.
53. Zhao Y, Shen Y, Ma S, Luo J, Ouyang W, Zhou H, Tang R, Wang M (2019) Production of 5α-androstene-3,17-dione from phytosterols by co-expression of 5α-reductase and glucose-6-phosphate

dehydrogenase in engineered *Mycobacterium neoaurum*. Green Chem 21(7):1809–1815.

54. Zhou X, Zhang Y, Shen Y, Zhang X, Zan Z, Xia M, Luo J, Wang M (2020) Efficient repeated batch production of androstenedione using untreated cane molasses by *Mycobacterium neoaurum* driven by ATP futile cycle. Bioresour Technol 309:123307.

Figures

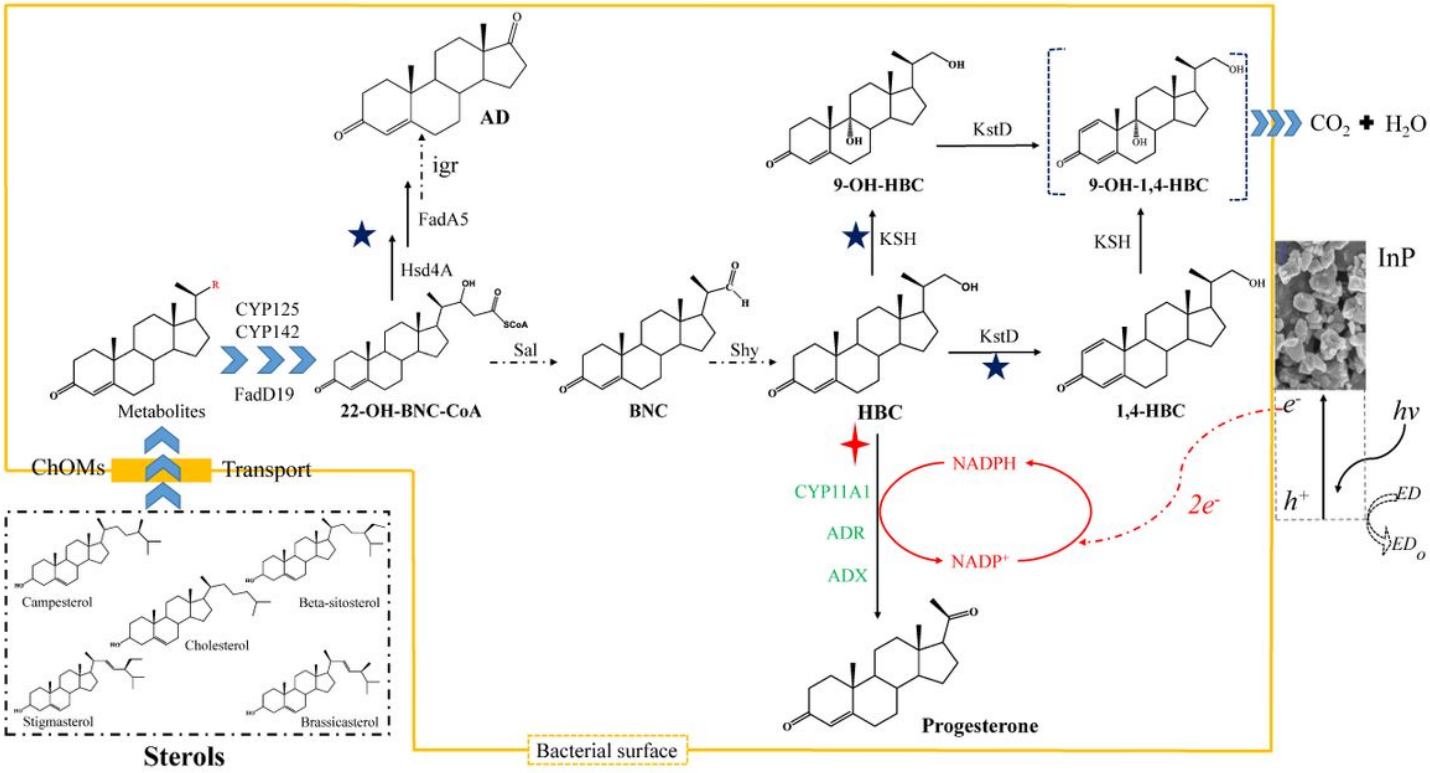

Figure 1

Progesterone biosynthesis schematic in InP-(*M. neoaurum*) biohybrids. The schematic depicts an abbreviated overview of the progesterone pathway, beginning with this work's carbon source sterols. The blue star shows these branch points or building blocks were deleted in this study. The red cross indicates the focus of this study, which is the putative next pathway as performed by the cytochrome P450 (CYP11A1) and its reductase partners. The surface shows the process of cellular NADPH regeneration by photogenerated electrons from InP nanoparticles. h^+: electron hole, e^-: electron, ED: electron donors, ED_o: oxidized electron donors, ChOMs: cholesterol oxidase transport system.

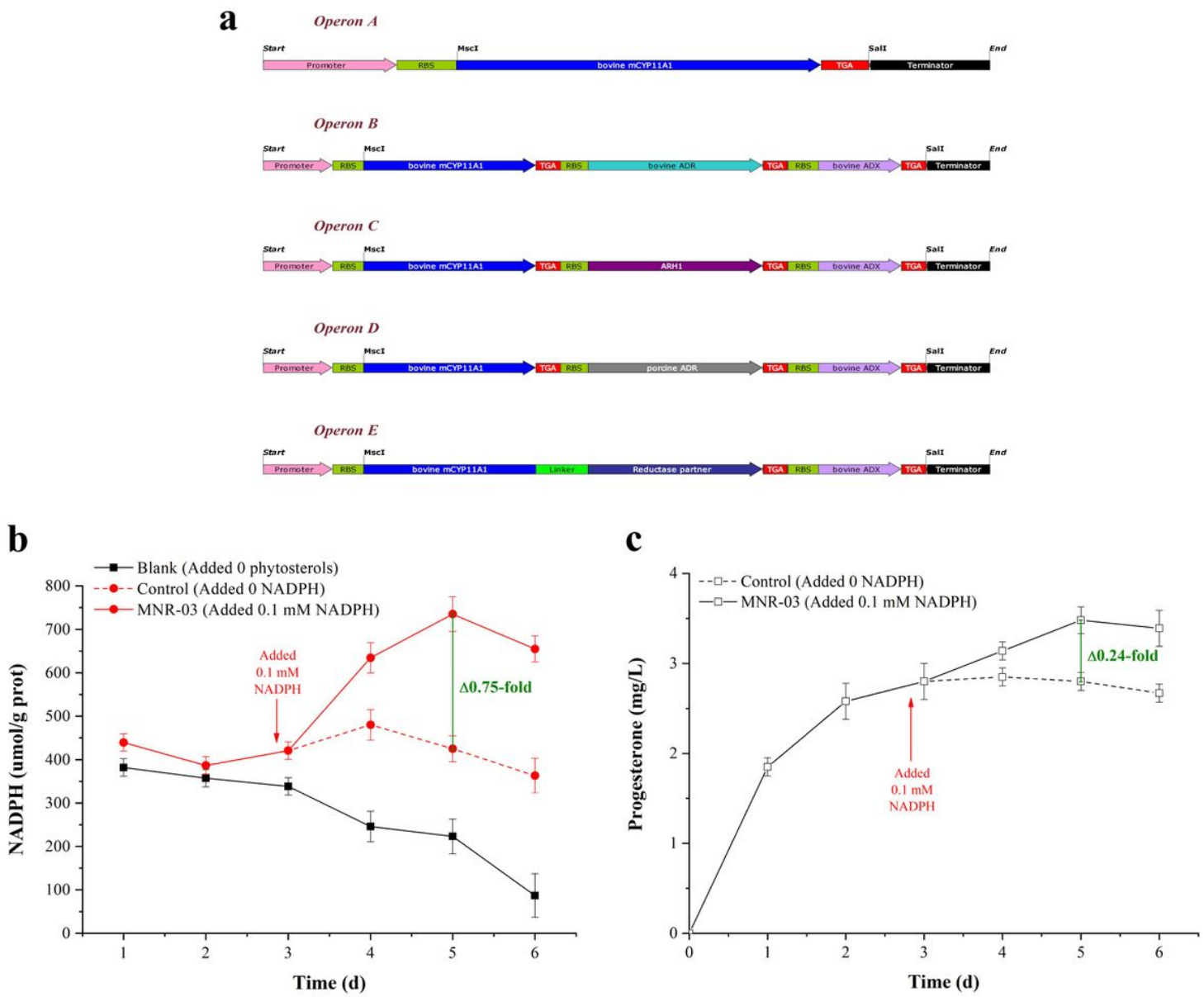

Figure 2

Overcoming the interdependence of P450 catalysis between CYP11A1 and reductase partners in *M. neoaurum*. (a) Overview map of bacterial operon mainly contains genes *cyp11a1* and its partners. RBS: GGAGGAA, Linker (L): $(GGGGS)_2$. (b) Intracellular NADPH concentration of MNR-03. (c) Corresponding to progesterone titer of the Fig. 2b. The value of the control group was treated as unit one on fermentation of the fifth day. All NADPH assays were performed before bacterial sludge were washed 3 times using PBS buffer and ddH_2O, respectively.

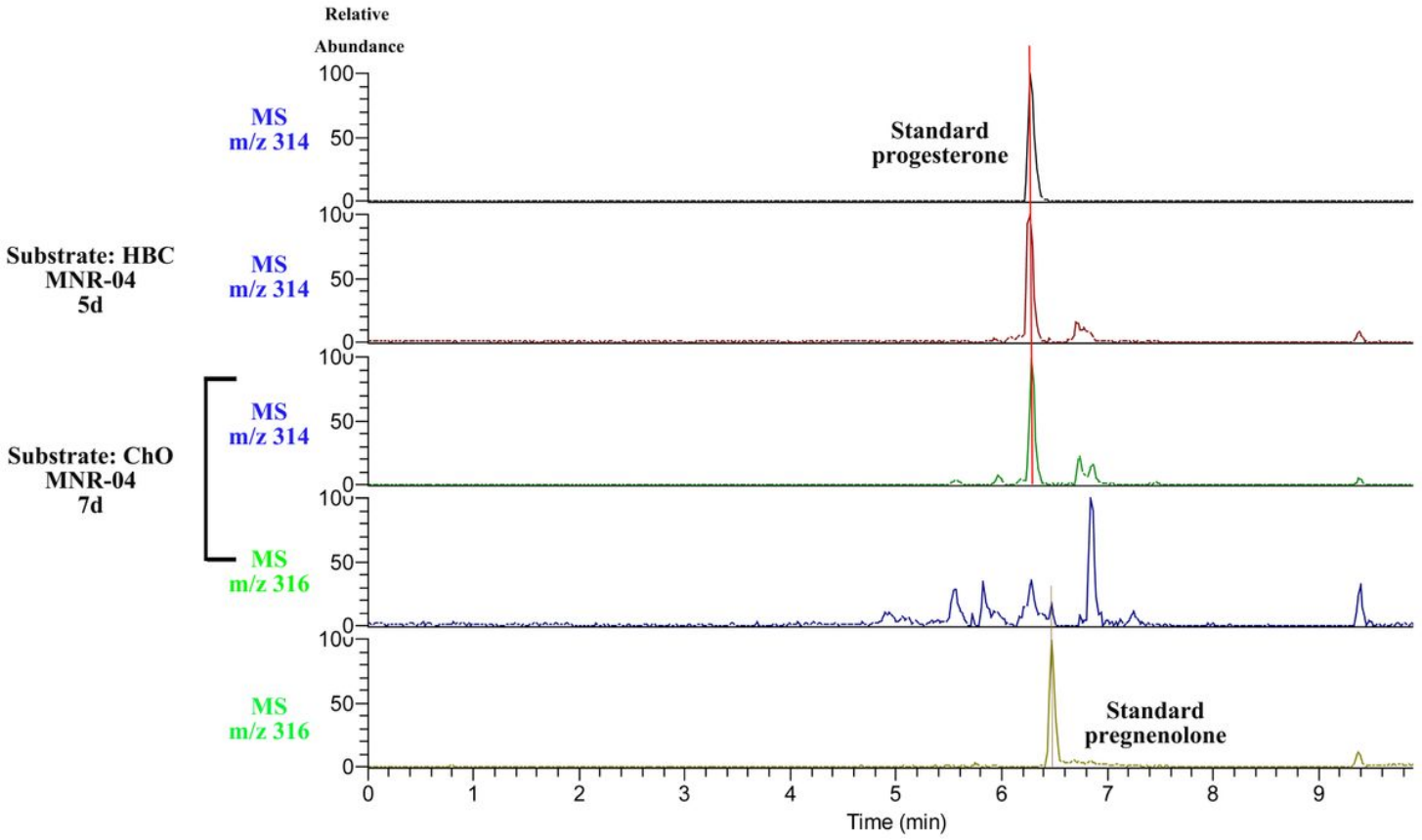

Figure 3

Analysis of products by high resolution mass spectrometry. The substrates HBC and cholesterol (ChO) were biotransformed by MNR-04 fermentation, respectively.

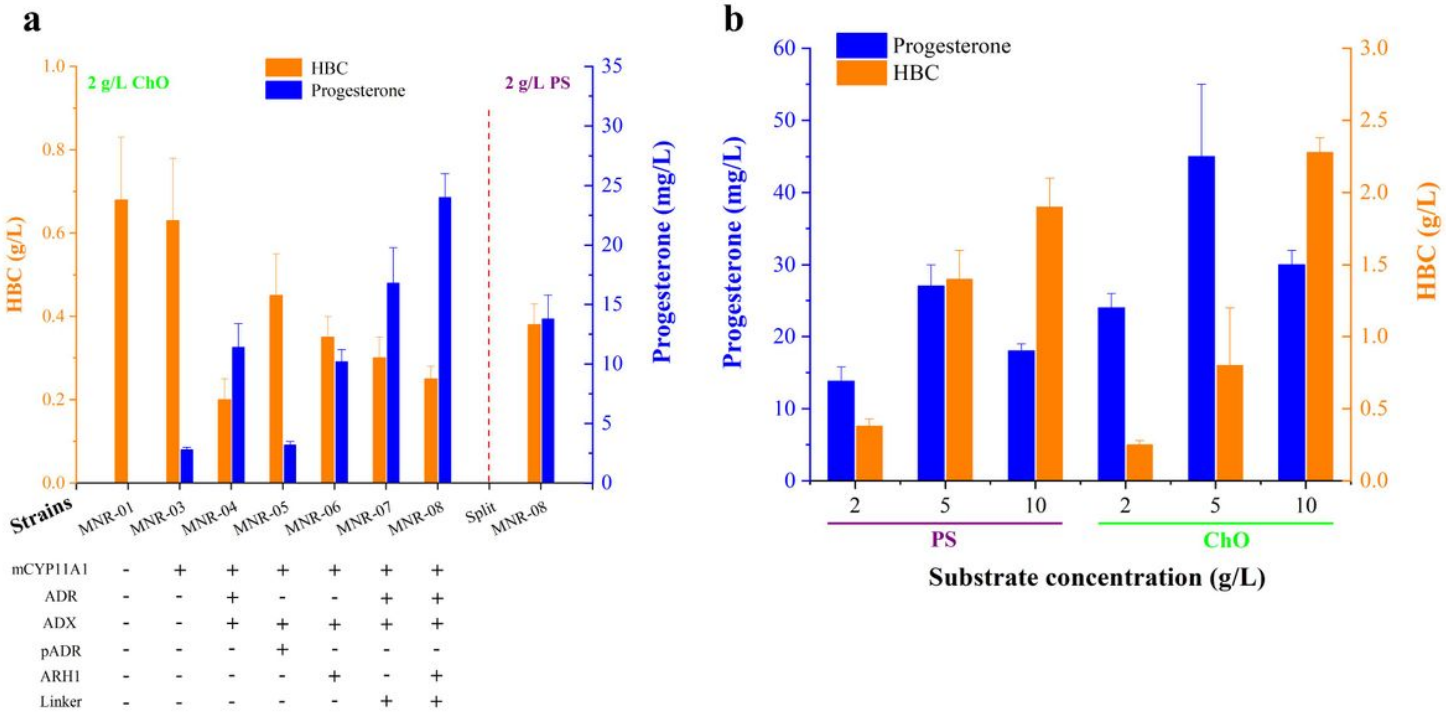

Figure 4

(a) P450 module optimization screen. For strain details, please see appendix, Table S1. **(b) The effect of substrates on progesterone production in pH 7.4 PBS by 20 g/L resting MNR-08 conversion for 5 days.**

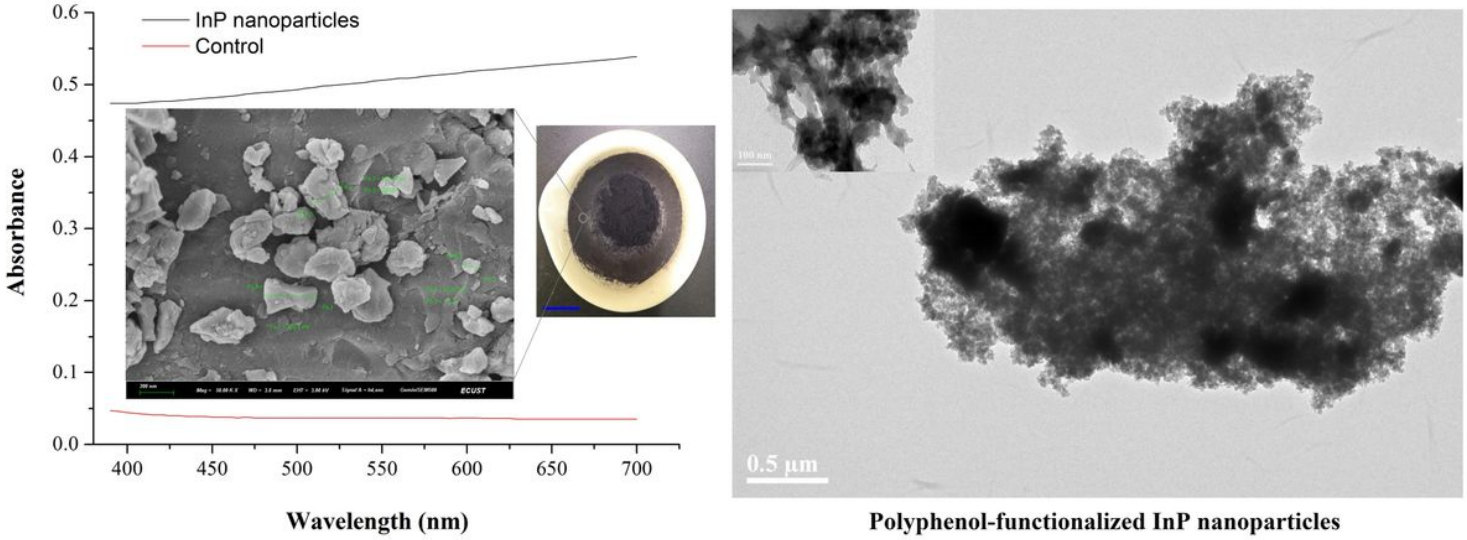

Figure 5

Characterization of InP nanoparticles. (a) UV-Vis spectrum of InP nanoparticles suspension in ddH2O, and the control was spectrum of ddH2O. SEM image shows the morphology of InP after grinding and its size is distributed in 20-350 nm with less than 500 nm. Blue scale bar is 1 cm. (b) TEM image shows that InP nanoparticles were functionalized via (tannic acid)-based coating. Tannic acid and InP form supramolecular networks on the surface of the nanoparticles resulted in InP is negatively charged.

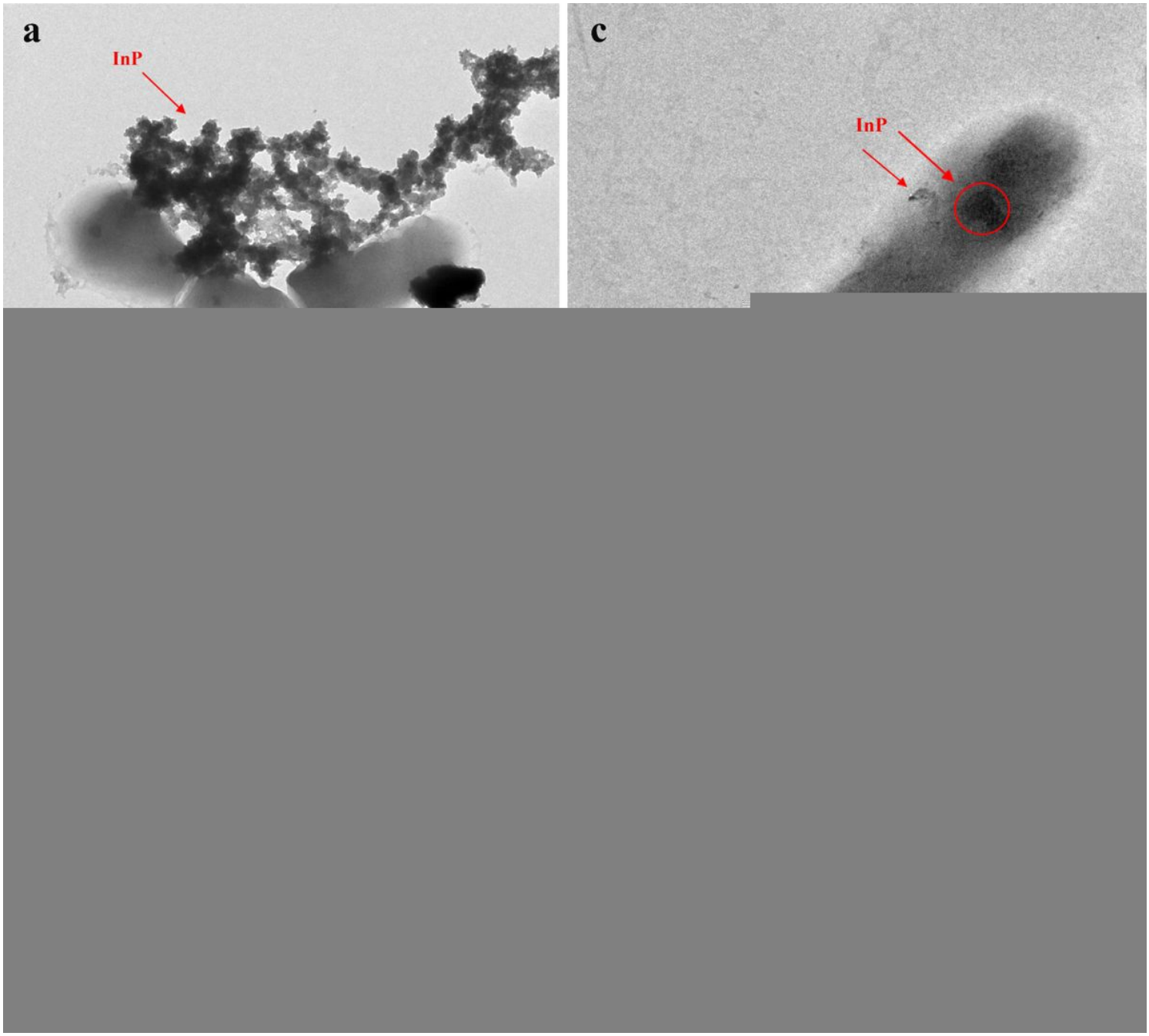

Figure 6

Characterization of *M. neoaurum*-InP biohybrids. TEM images show the overview of biohybrids, and InP of negative charges was adsorbed on the surface of MNR-08 with positive charges. The a, b, and c show the assembly results of InP and 20 g/L MNR-08 with different contents, respectively. (B) Schematic representation of the biohybrids based on the electrostation.

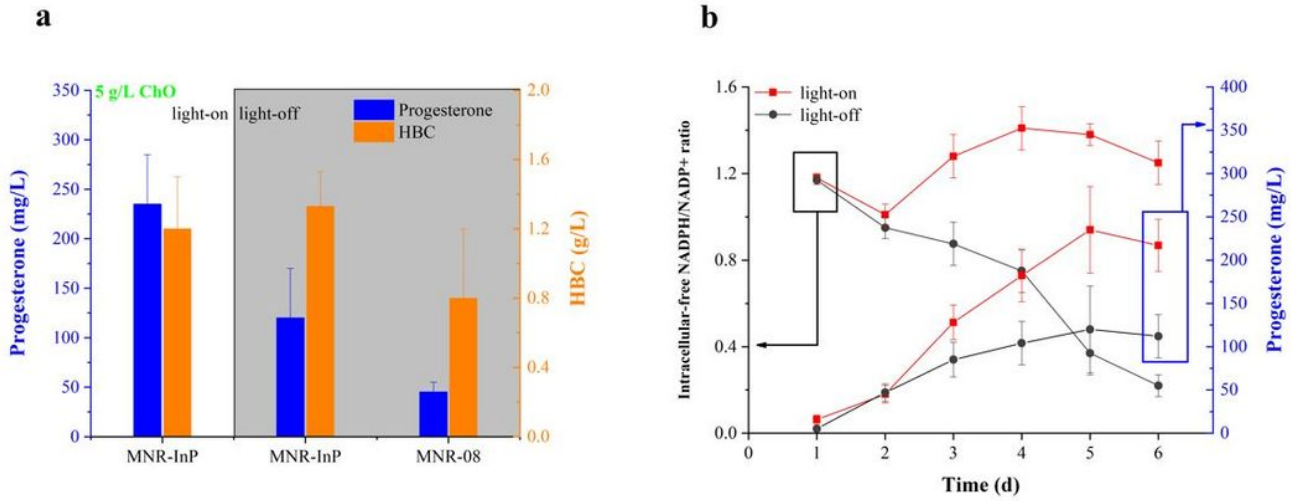

Figure 7

Improved progesterone production by light-driven NADPH regeneration. (a) Comparison of steroid titers in MNR-InP biohybrids and (MNR-08)-only resting conversions for 5 days in the flasks with light-on and light-off conditions. (b) Cytosolic-free NADPH regeneration and progesterone production profiles in light-on and light-off conditions.

Supplementary Files

This is a list of supplementary files associated with this preprint. Click to download.

- AbstractGraphic.docx
- Supportinginformations.docx